Tethys, 6, 81–100, 2009
Journal of Weather & Climate of the Western Mediterranean
www.tethys.cat
ISSN-1697-1523
eISSN-1139-3394
DOI:10.3369/tethys.2009.6.06

Journal edited by **ACAM**
(Associació Catalana de Meteorologia)

Study of the hailstorm of 17 September 2007 at the Pla d'Urgell. Part two: meteorological analysis

N. Pineda[1], **M. Aran**[1], **A. Andres**[1], **M. Busto**[1], **C. Farnell**[1] **and M. Torà**[2]

[1]Servei Meteorològic de Catalunya, c/Berlín 38-46 08029 Barcelona
[2]Agrupació de Defensa Vegetal de les Terres de Ponent

Received: 12-III-2009 – Accepted: 4-VIII-2009 – **Translated version**

Correspondence to: npineda@meteo.cat

Abstract

On 17 September 2007 a heavy hailstorm hit the Pla d'Urgell (Urgell Plain), with hailstones larger than 5 cm in diameter and 81 hailpads hit; unusual, given that hail in the area is usually smaller in diameter and size (7 hailpads affected on average). The first part of the study (Farnell et al., 2009) deals with the effects of the hailstorm on the surface, based on extensive fieldwork and the data obtained from hailpads in the area. This second part of the hailstorm study examines the episode from a synoptic point of view and from the observations recorded with the various tools available to the Servei Meteorològic de Catalunya (Meteorological Service of Catalonia): Meteosat images, data from the radar network and lightning records obtained from the atmospheric electrical strikes detection network. At the synoptic level, it is noteworthy that the episode occurred in conditions prone to produce graupel/hail in the area, with the presence of a wide trough at high levels associated with a low pressure system in Scandinavia. Analysis of the Meteosat images indicates that the storm core that produced the hailstorm was part of a mesoscale convective system. Originating in the center of the Iberian Peninsula, it moved to the NE, affecting Catalonia in the afternoon and later moving to southern France, where it also left heavy hailstorms. Study of the radar data reveals the presence of a hook-shaped storm during the hail. Despite this, this storm can not be defined as a supercell (a mesocyclone is not detected). On the other hand, it is observed that the maximum vertical developments occurred in the area where larger hailstones were detected. From the monitoring of the atmospheric electrical activity of the episode, we can highlight the high frequency of lightning generated by the storm. These results reinforce the conclusions of the analysis of the Meteosat and radar images on the severe nature of the storm.

Key words: hailstorm, inhibition, convective, V-notch, lightning

1 Introduction

The study of storms with graupel and/or hail is complex, as the phenomenon must be analyzed at different working scales, from synoptic to local. While the meteor affects a very small area in a short space of time, the storm that generates it has a life cycle and an extension of a higher magnitude. At the same time, these storms usually are part of a well-organized convective system of mesoscale dimensions.

The lower part of the Ebro valley is one of the areas most affected by graupel/hail in the Iberian Peninsula (Sánchez et al., 2003) and has been the subject of numerous studies related to this meteor (e. g. Pascual, 2002; Tudurí et al., 2003; Ceperuelo et al., 2006; Aran et al., 2007). At a synoptic-scale, convective development in the region has been favored by the release of latent instability due to a strong heating of the earth (Font, 1983). However, more recent studies based on numerical simulations (e. g. Ramis et al., 1999; Tudurí et al., 2003; García-Ortega et al., 2007) highlight the importance of the presence of a mesoscalar low of a thermal origin in the development of hailstorms in the Ebro valley.

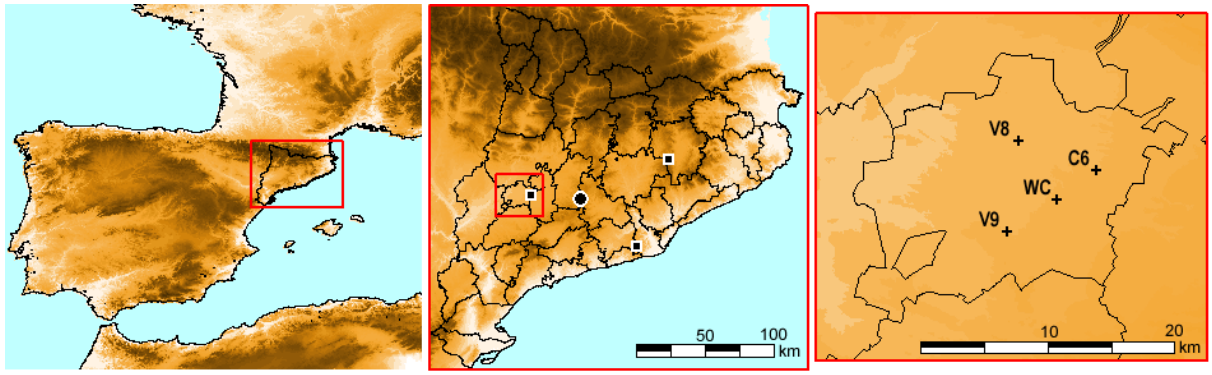

Figure 1. (a) (left) Area of interest within the framework of the Iberian Peninsula. (b) (right) area of interest in Catalonia. Radar of the *Xarxa de Detecció de Descàrregues Elèctriques* (atmospheric electrical strikes detection network) (squares). (c) District of Pla d'Urgell with the AMS analyzed in the region: El Poal (V8), Castellnou de Seana (C6), Golm (WC) and Miralcamp (V9).

The objective of this study is to perform a meteorological analysis at several levels of the episode that took place on 17 September 2007, the strongest since 1990 according to data collected in the area. It affected the districts of Segrià, Pla d'Urgell, Urgell and Noguera. The study focuses on the Pla d'Urgell, which was almost hit in its entirety by the hailstorm, and about which there is a significant set of observations on the ground. The analysis of these data is presented in the first part of this study (Farnell et al., 2009) and it is useful when interpreting the data obtained from remote sensing tools. In this second part of the study, after presenting the data used, we analyze the synoptic environment and the conditions of instability through radiosonde data. Then, at a mesoscalar level, the thermal boundary and the passing of the front is analyzed using the mesoscale convective system with the help of images from the Meteosat satellite. Next, we analyze the internal structure of the storm and its life cycle, from radar observations and records of lightning. Finally, we present the conclusions of the study.

2 Data

The available data for this study come primarily from the weather observation systems of the *Servei Meteorològic de Catalunya* (Meteorological Service of Catalonia, SMC). The satellite images used correspond to the water vapor channels (6.2 μm) and the thermal infrared (10.8 μm) of Meteosat-9 (M-9). The radar data come from the SMC radar of La Panadella (N 41°36'06"; E 1°24'10"; Alt: 825 m) located approximately 50 km east of the study area (Figure 1). The collection of radars that form the Meteorological Radar Network (XRAD) of the SMC operate in C band (5.600 to 5.650 MHz) and are of a Doppler type. Bech et al. (2004) detail the particularities of XRAD. The lightning data come from the Lightning Detection Network (XDDE) of the SMC, which is composed of three SAFIR detectors (Richard and Lojou, 1996) (Figure 1). This lightning detection system can detect both cloud-to-cloud lightning (CC) and cloud-to-ground lightning (CG), as the detection stations combine a sensor with a very high frequency (VHF, 108-120 MHz) that detects CC with a low frequency sensor (LF, 300 Hz to 3 MHz), which discriminates the detected discharges corresponding to cloud-to-ground lightning (CG) and measures certain electrical characteristics (polarity, peak current, etc.). More details about the XDDE can be found in Pineda and Montanyà (2009).

On the other hand, the data from the SMC radiosonde were used, which was launched in Barcelona (N 41°37'12"; E 2°12'00"; Alt: 96 m) at 00 and 12 U.T.. Data from the Murcia radiosonde (N 38°00'00"; W 4°10'12"; Alt: 62 m) of the Spanish Meteorological Agency were used in addition, since the Zaragoza radiosonde was not available. Maps derived from the 163 automatic meteorological stations (AMS) of the SMC, as well as the temporal evolution of the records of the four AMSs located at the Pla d'Urgell, are also included in the study.

3 Environmental scan summary

A depression located in the northern half of the Iberian Peninsula was the trigger for the formation of severe storms in Catalonia early in the afternoon of 17/09/2007 (Figure 2a). At 500 hPa there is a trough that stretches from the North Sea to Galicia (Figure 2b). To analyze in detail the main synoptic settings and the general flows in the area of interest, we used the images of the water vapor channel of the M-9 at 00 U.T. and at 12 U.T. of the day in question. The first image (Figure 3a) reveals a secondary low pressure system in the north of Portugal with relative maxims of southerly wind at its eastern sector. The dynamic ridge lies further to the east near the Mediterranean coast and oriented NW-SE. At 12 U.T. (Figure 3b) this relative low is located on the north of the Iberian Peninsula and moves towards Catalonia. The new location and orientation of the wind maxims generate an area of diffluence at the north of Navarra and Aragon, where convective cells with a marked vertical development (round

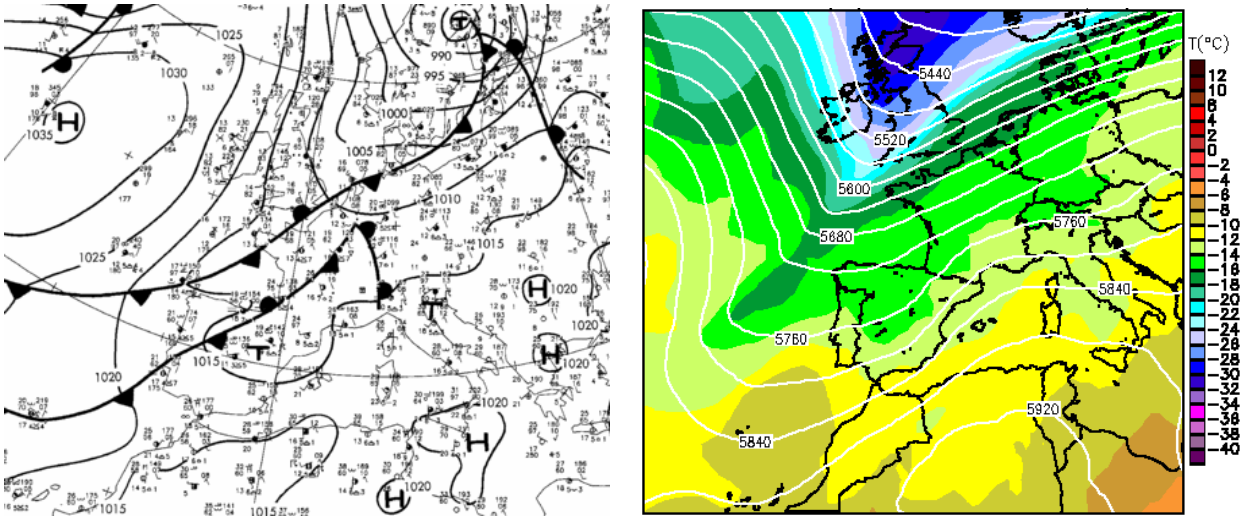

Figure 2. (a) (left) Reanalysis of the pressure on surface and (b) (right) analysis of the geopotential and temperature at 500 hPa at 12 U.T. Of 17/09/2007 from the Global model of the Deutscher Wetterdienst.

Table 1. Data from the radiosonde in Barcelona on 17/09/2007 at 00 U.T. until 00 U.T. on 18/09/2007. Temperature (T) and frost point (T_d) for 300, 500, 700, 850 and 925 hPa and wind speed and direction at 300 hPa.

Level	Variable	17/09/2007 00 U.T.	17/09/2007 12 U.T.	18/09/2007 00 U.T.
300 hPa	T (°C)	-41.5	-41.7	-41.5
	Wind dir. (°)	240	230	265
	Speed. (kts)	34	48	53
500 hPa	T (°C)	-12.1	-13.5	-13.7
700 hPa	T (°C)	5.8	8.4	3.2
	T_d (°C)	-2.2	-19.6	2.2
850 hPa	T (°C)	17.4	17.0	16.4
	T_d (°C)	3.4	9.0	6.4
925 hPa	T (°C)	19.0	17.4	19.2
	T_d (°C)	13.0	16.9	15.7

and white signal brighter in the images of the water vapor channel, Figure 3) are already observed. The ridge, displaced further to the east, is strengthened and enters into southern France. This synoptic configuration and its evolution is similar to that observed in other episodes of hail affecting the area of the Lleida plain (Tudurí et al., 2003; Ceperuelo et al., 2006; Aran et al., 2007). The presence of a trough at high levels associated to a fall in the north of the Iberian Peninsula is a recurring situation in hailstorms in Lleida on more than 38% of days, according to the climatology of Pascual (2002) during the period 1995-1999.

With the reanalysis at 500 hPa at 12 U.T. (not shown) a cold core of the secondary low with -16°C is detected on Madrid. From the reanalysis of 925, 850 and 700 hPa (only the 700 hPa thermal field is shown, Figure 4) we can gather that the air mass on the Mediterranean coast was damp below approximately 700 hPa, depending on its location; the content of precipitable water mass was about 70% of the total according to the radiosonde data in this stratus. Above this level, delimited by a thermal inversion, there was a much drier stratus: on Murcia, the frost point was -28.4°C with 5% of relative humidity and on Barcelona there was a temperature of -19.6°C with 12% of relative humidity (Figure 5). Table 1 shows the time evolution of temperature (T) and frost point (T_d) on Barcelona at different levels. The presence of a damper mass on the level of 925 hPa is highlighted, with values for the frost point depression at 0.5°C at noon. In the analysis of this level (not shown) we can see a progressive increase in humidity from the SE to the NE of the Peninsula. The subsidence associated to the ridge and, possibly, the contribution of the warm advection of the wind in the southeast determined the characteristics of this air mass. According to data from the radiosonde, the air mass on Barcelona at 12 U.T. was similar to that presented on Murcia twelve hours earlier, as shown in Figure 5. In twelve hours the ridge moved from Murcia to Barcelona (Figures 2 and 3). The

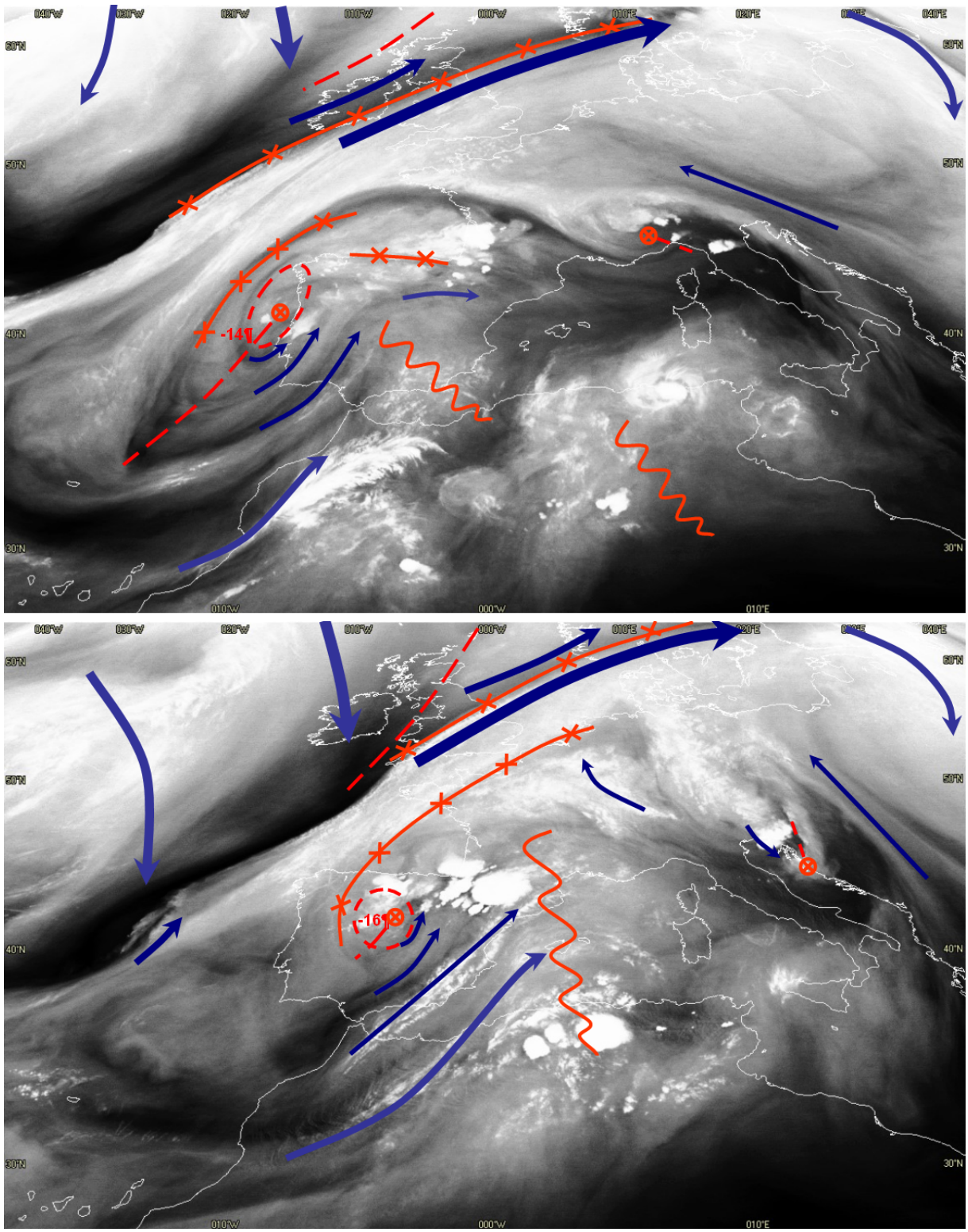

Figure 3. Image analysis of the Water Vapor Channel of the satellite M-9 (a) at 00 U.T. and (b) at 12 U.T. on 17/09/2007. Symbols: cold core (circle), center of rotation (cross in circle), axis of the trough (broken line), ridge (winding line), deformation zone (line with crosses), maximum wind (arrows).

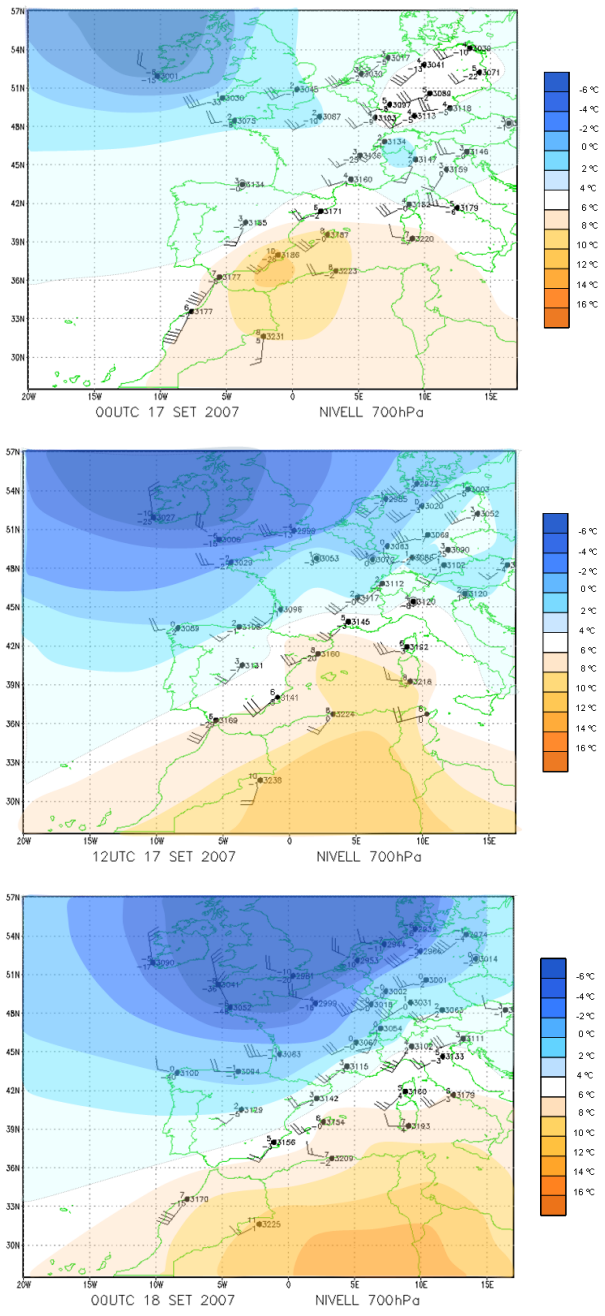

Figure 4. Reanalysis of temperature (°C) at a level of 700 hPa (a) (top) 17/09/2007 at 00 U.T. (b) in between 17/09/2007 at 12 U.T. (c) below 18/09/2007 at 00 U.T.

inversion of the subsidence that was formed on Barcelona at 12 U.T., although not very strong, was enough to inhibit convection. Moreover, the presence of a drier and colder stratus above the warm and damp mass favored an increase in potential instability.

In order to analyze the conditions of instability in the area of Lleida, some indexes obtained from the Barcelona radiosonde were used. In this kind of synoptic situation, with southeastern advection throughout the Mediterranean coastal strip, the hypothesis that the characteristics of the air mass in the Lleida area are similar to those of Barcelona is posed (Aran et al., 2007). A first index analyzed in order to evaluate whether the inversion could be broken was that the convective inhibition (CIN) was -153 J kg^{-1}, high enough to prevent widespread convection but not enough to break the inhibition and favor local convection (Davies, 2004). Another index used to measure inhibition due to inversion is the Lid Strength Index (LSI) (Graziano and Carlson, 1987). These authors observed that in situations of strong convection the LSI took values between 1 and 2 K, with values reaching, in some cases, up to 3 K. However, LSI values below 1 K correspond to situations where there is no inhibition, while above 3 K convection is completely inhibited. In Barcelona the LSI at 12 U.T. was 3.1 K; therefore it was possible to initiate convection in places where there was not enough forcing. In fact, it was only when the low was located to the west of Catalonia that there was an additional forcing to initiate convection, along with other mechanisms such as daytime heating and the front of gusts typical of convective cells with moderate to strong precipitation.

The Lifted Index (LI), the Total Totals (TT) and the Convective Available Potential Energy (CAPE) are among the indexes most employed to analyze convection. In this episode, the CAPE, an estimate of the potential energy available for the development of convection, was 1571 J kg^{-1}, similar to that obtained in other episodes of hail analyzed in the Lleida area (Tudurí et al., 2003; Ceperuelo et al., 2006; Aran et al., 2007). The LI also had high values of -5.4°C and the TT as well, with values of 51.1°C. The temperature difference between 500 and 850 hPa was 30.5°C, which was also favorable to convection.

So on this day, on the outskirts of Barcelona there were only weak precipitation cells late in the afternoon. The inhibition at 700 hPa was broken in the west from 13 U.T. favoring localized convection with large vertical development. The storms were organized along a line in the pre-frontal area and moved to the northeast. At the end of the day the front passed, the warmest mass moved towards the Mediterranean (Figure 4) and the convection was dissipated throughout the Iberian Peninsula.

To determine the type of precipitation it is necessary to analyze the vertical profile of temperature and wet-bulb temperature. The freezing level of the wet-bulb thermometer at 12 U.T. was at 2888 m, a critical value, since below 2 km convection is unlikely because the layer is too cold (Holleman, 2001). When the freezing level is very high (above 3000 m) hailstones make a long journey before reaching the surface, during which they melt and shrink in diameter. However, according to data from the radiosonde of Barcelona, the top of the cloud was at approximately 13 km (values up to 15 km were observed with radar in the area of Pla d'Urgell), therefore, the iced cores within the cloud were inside updrafts in about 12 km. These updrafts enabled the graupel core to grow, either by impact with other cores or by pick-

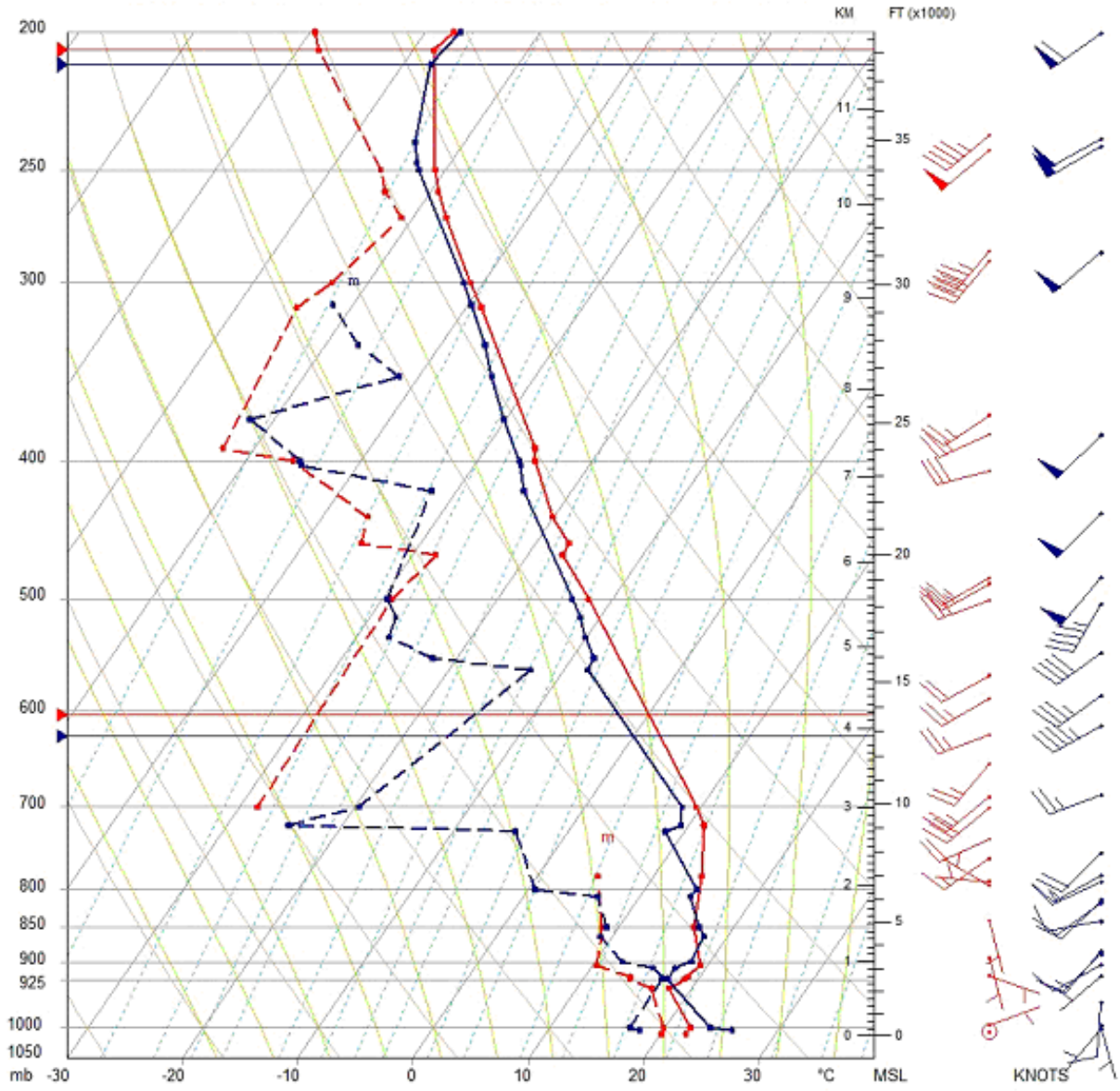

Figure 5. Comparison of the radiosonde of Murcia on 17/09/2007 at 00 U.T. (red) and Barcelona on 17/09/2007 at 12 U.T. (blue).

ing up humidity from the environment. These conditions are prone to great growth in the graupel cores, as proven on the surface in this episode, where hailstones up to 5 cm were observed (Figure 6).

4 Mesoscale analysis

4.1 Thermal boundary and passage of the front

In addition to synoptic forcing due to the passage of a frontal system (Bluestein, 1986), in some cases the interaction of a convective cell with a thermal boundary, either in the warm sector of the frontal system or due to a gust generated by the precipitation itself, may promote an intensification of the convection within the convective system (Atkins et al., 1999; Corfidi, 2003). To put the thermal boundaries in Catalonia we used the thermal spatial distribution of solar irradiance (Figure 7), and of the temperature (Figure 8) recorded in the AMS. In those days of September the solar irradiance was characterized by high values above the average normal peak values of the past 10 years (in the station of Castellnou de Seana 826 W m^{-2} were registered, compared to the 689 W m^{-2} on average). On the day of the hailstorm the day warming in the area of the Lleida plain was elevated with a warm core over the area of Pla d'Urgell (30°C). At 14 U.T. the cold air discharge due to the precipitation of convective cells (the temperature drop was about 10°C in 2 hours

Figure 6. Graupel and hailstones observed at several points of the study area. Photos courtesy of Xavier Coll and Francesc Farnell.

at all the stations of the area) and the cooling due to the increasing cloudiness accentuated the thermal gradient in that area (Figure 8) reaching values of 10°C in 40 km (from the border between Aragon and the Segrià and the Pla d'Urgell). At that time there was an intensification of the convective system in the Pla d'Urgell area. The higher intensities in Catalonia were recorded between 15 and 15:30 U.T. in this region; during this interval 24.7 mm were registered in El Poal, 19.6 mm in Golmés and 11.4 mm in Miralcamp.

To detect the front's passage, we analyzed the temporal evolution of temperature at the Pla d'Urgell stations on 16, 17 and 18 September, before and after the day of the hailstorm. The temporal evolution of temperature at the stations in the Pla d'Urgell shows cooling due to the precipitation downdrafts and the subsequent passage of a cold front. A change of air mass was also detected. On the 18th temperatures were lower despite the fact that the solar irradiance was similar to previous days. The passage of the front is visible in the analysis of the evolution of wind direction. Hours before the hailstorm there was an easterly sustained wind, in general, reaching moderate levels of intensity (Castellnou de Seana, 5.9 m s^{-1} at 14:30 U.T., Figure 9). The maximum gusts were also moderate (between 8.3 and 15.6 m s^{-1}) and occurred near 15 U.T. Once the storm ended, the wind turned west. Finally, with respect to atmospheric pressure, it gradually fell from the 16th until 14:30 U.T. of the 17th, the time of the hailstorm. At the station of Castellnou de Seana it decreased in 6 hPa between 9 and 14 U.T. (Figure 9). Subsequently, the pressure gradually increased.

4.2 Mesoscale Convective System

This section presents the results of the analysis of the images of the M-9 thermal infrared channel (IT) in monitoring the convective cells that affected the study area and examines whether they formed part of a mesoscale convective system (MCS). We worked with two thresholds of cloud-top brightness temperature, specifically -32°C (TB-32) for contouring the MCS (Maddox, 1980; Maddox et al., 1986) and -52°C (TB-52) to define the convective zone of the system (Augustine and Howard, 1988, 1991). That threshold has proven to be appropriate for our latitudes according to works in identification of the MSC in the Iberian Peninsula, such as Sánchez et al. (2001) or Correoso et al. (2006). The method proposed by Jirak et al. (2003) was also used to classify the storm system.

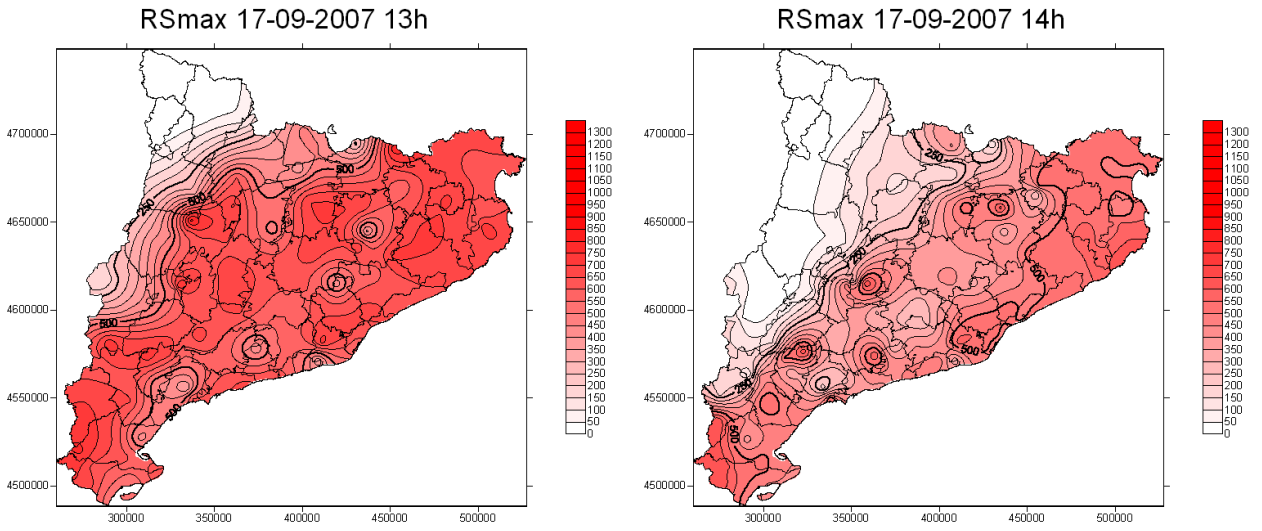

Figure 7. Maps of solar irradiance (in W m^{-2}) from 17/09/2007 at (a) (left) 13 U.T. and (b) (right) 14 U.T., obtained with the AMS.

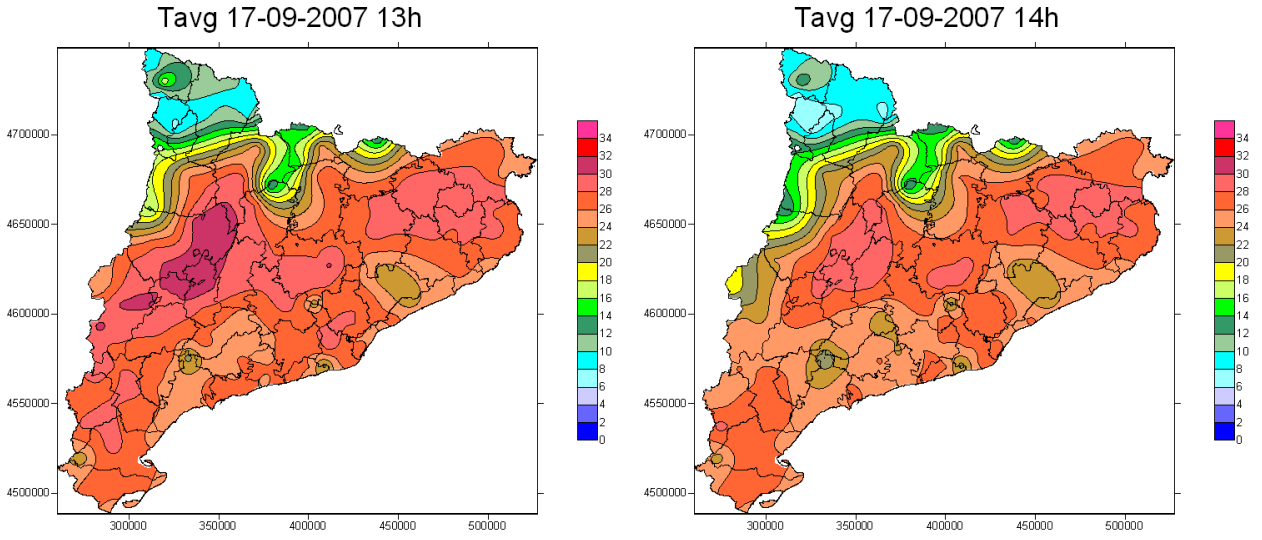

Figure 8. Maps of temperature (in °C) from 17/09/2007 at (a) (left) 13 U.T. and (b) (right) 14 U.T., obtained with the AMS.

The IT image analysis revealed that the system showed a continuous area with a TB-52 in an area of over 50.000 km^2 over 6 hours and may be classified as a MSC. Jirak et al. (2003) defined 4 types of MSC, according to duration and eccentricity (defined as the division between major and minor axes of the continuous area with TB-52, at the time of maximum extension). In this MSC eccentricity was 0.72, and the longer duration was 6 hours. According to this classification we can speak of a mesoscale convective complex (MCC).

The convective system begins to be displayed (it presents pixels with TB-52) at 06 U.T., in the southwest of the Iberian Range, in the vicinity of Guadalajara. From 07 U.T. pixels with TB-52 are already observable in the center of the storm core, moving toward the NE. The system continues to grow as it moves, and at 10 U.T. it is already in the vicinity of Zaragoza, when cloud-top temperatures below -65°C can be observed. As at first, it is a linear structure; as it grows it takes a more circular shape, becoming an ellipse of low eccentricity at 10 U.T. Until now, the system consisted of a single cell, but from 10:15 U.T. a series of cores in the rear flank of the main cell began to build-up, and as the system continued moving toward the NE, these cells grew and eventually became part of the main system. Between 12 and 13 U.T., the system merges with a series of cells formed in the left flank, over the Basque country, a fact which greatly increases its area (Figure 10). At 13 U.T., the system covers a large part of the central and eastern Pyrenees, covering an area of over 50.000 km^2. The

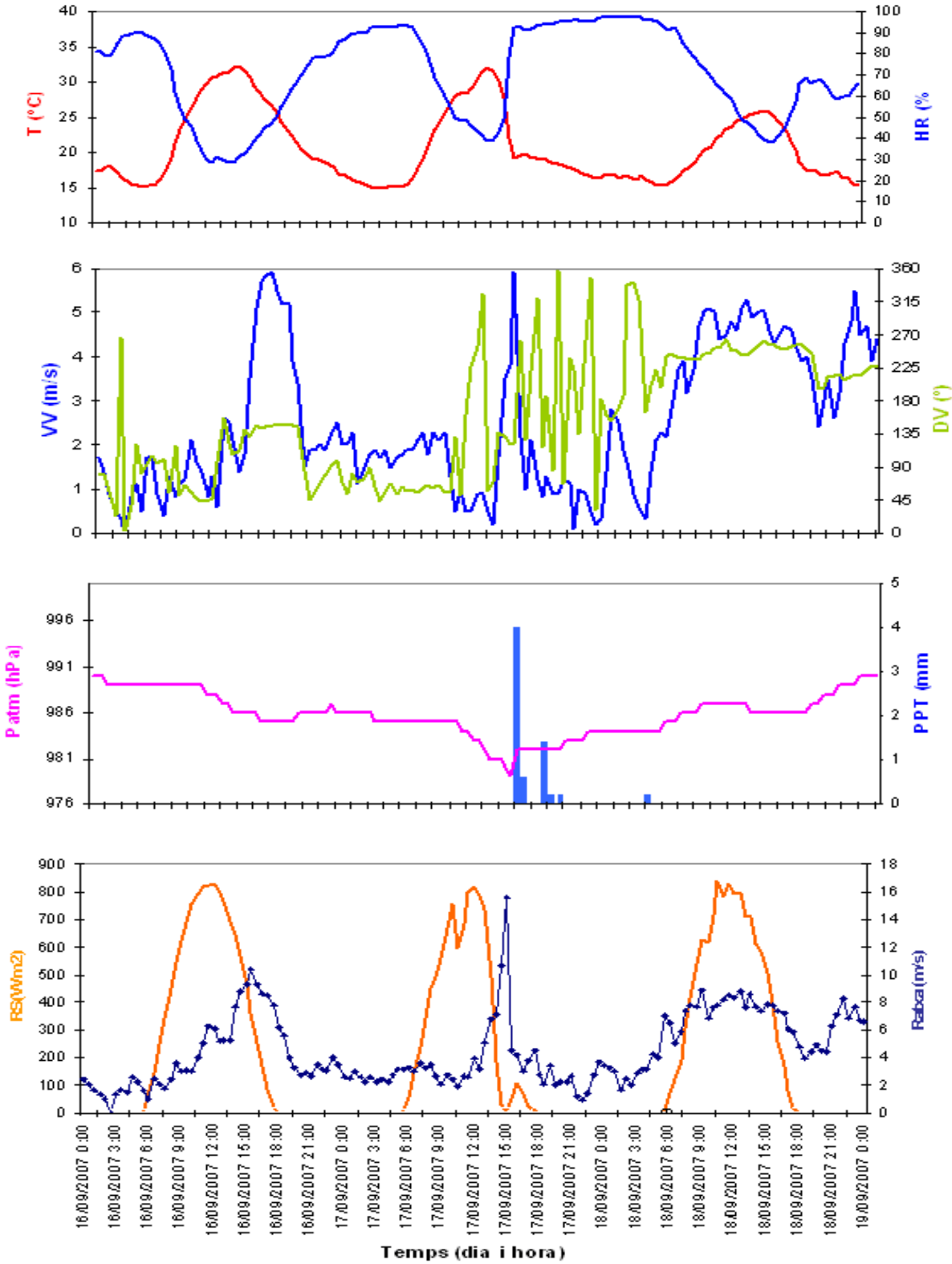

Figure 9. Evolution of different meteorological variables at Castellnou de Seana meteorological station during the period 16/09/2007 00 U.T. - 19/09/2007 00 U.T. Temperature (T), relative humidity (RH), wind speed at 10 m of altitude (VV), wind direction at 10 m of altitude (DV), precipitation (PPT), atmospheric pressure (P_{atm}), solar radiation (RS) and wind gusts at 10 m (*Ratxa*).

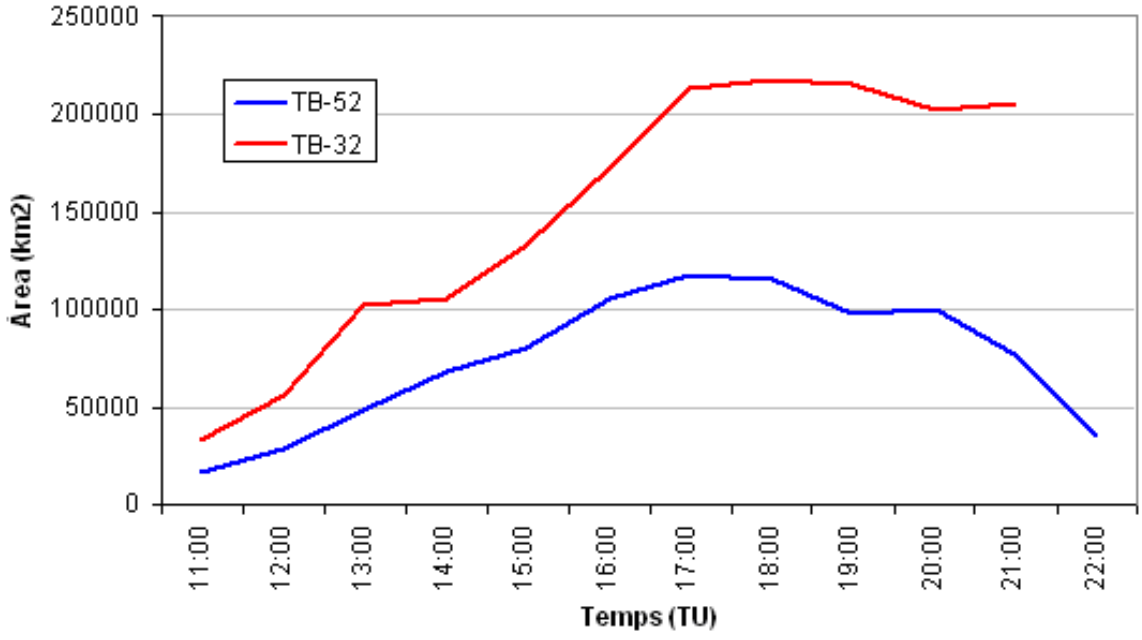

Figure 10. Evolution of continuous area (km^2) with cloud-top brightness temperature in the IT channel of the M-9 below -32°C (TB-32) and -52°C (TB-52).

system reaches a size over 100.000 km^2 from 16 U.T., once located over Catalonia and a large part of southern France, while maintaining a dimension larger than 50.000 km^2 until 21:30 U.T.

The storm cell responsible for the hailstorm in the Pla d'Urgell begin to become visible in the IT images of M-9 at 11:15 U.T., in the Zaragoza area, and it presents further development than all the ones that emerge in the rear flank of the main cell. Between 12 U.T. and 13 U.T., this cell merges with the most southern core of the MSC, crossing Catalonia from SW to NE between 13:30 and 18 U.T. Figure 11 shows the system's shape (area TB-52) in four periods of its life cycle. Figure 12 shows the IT colored image at 14 U.T., when the colder core is over the Pla d'Urgell.

Sánchez et al. (2003) analyzed 72 cases of storms with graupel/hail in the area of Lleida and found that in 37% of the cases there was MSC and in 5% of cases MCC. According to statistics, since 17/09/2007 MCC is quite rare in the region. Finally, it is noteworthy that half of the 4 MCCs detected by Sánchez et al. (2003) occurred in autumn, as in this case.

A more detailed analysis of the IT image at 14 U.T. shows a V-shaped feature, which is characteristic of severe storms (McCann, 1983; Adler and Mack, 1986), formed as a result of the interaction between strong updrafts and winds at middle-high levels. The V-shaped feature appears when the strong updrafts of the storm make the clouds penetrate in the lower stratosphere through the tropopause, creating overshooting tops (Heymsfield and Blackmer Jr., 1988). This intrusion into the stratosphere blocks the wind at high levels and forces the wind flow to diverge around the overshooting, creating a depression in the leeward (Fujita, 1978) (Figure 13). At 14 U.T. the anvil of MSC showed a V-shaped feature with the rounded apex typical of moderate stratospheric flow situations (Heymsfield and Blackmer Jr., 1988).

These V-shaped cloud structures also show the presence of a thermal dipole to the leeward of the anvil, which is another indicator of severe weather (Wang, 1997; Brunner et al., 2007b). The overshooting is identifiable with imaging techniques, combining information from the water vapor channels and thermal infrared (Kurino, 1996; Veciana et al., 2003). Brunner et al. (2007a, 2007b) developed an automatic identification method, in which they propose 5 conditions that must exist in images of GOES (geostationary satellite that covers the American area). These are i) Presence of overshooting: the difference in brightness temperatures of the water vapor channels (6.5 μm) and thermal infrared channel (10.7 μm) must be higher than zero. ii) The temperature of the coldest pixel of the overshooting zone must be lower or equal to 215 K. iii) The temperature difference between this cold pixel and its warm pair (depression to leeward, Figure 13) must be between 6 and 25 K. iv) The distance between this pair of pixels should be less than 20 km. v) The warm pixel must be within the smaller angle formed by the two arms of the "V" (Figure 14).

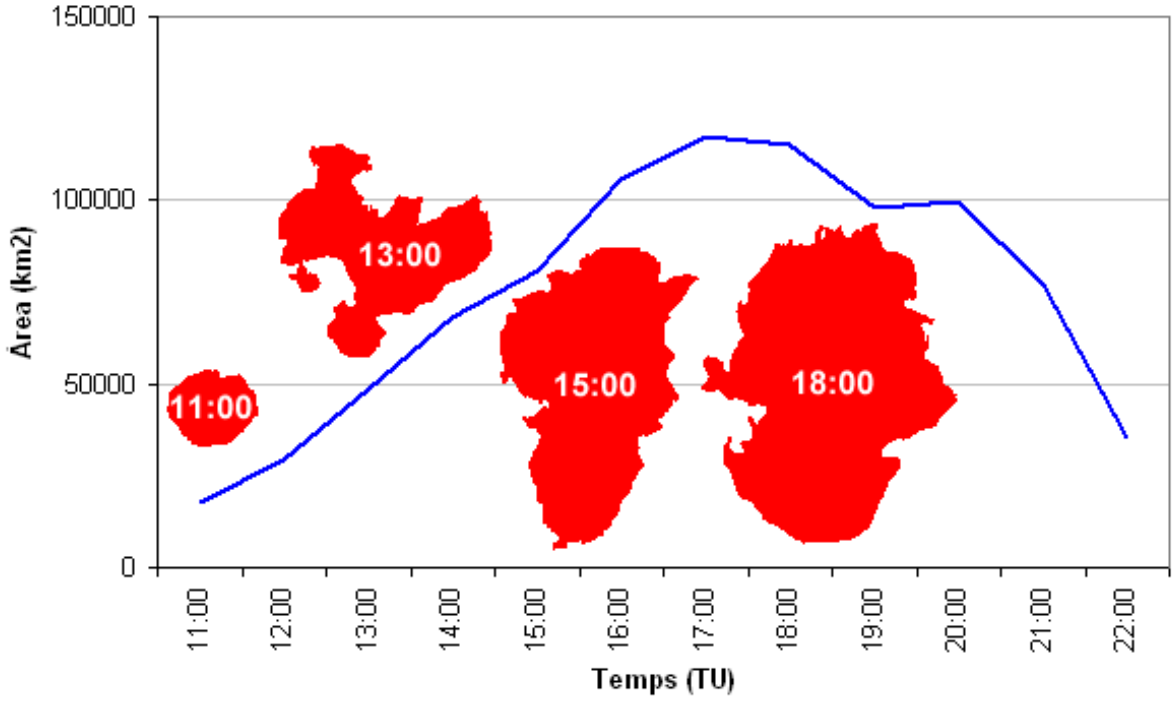

Figure 11. Evolution of continuous area (km^2) with cloud-top brightness temperature in the IT channel of the M-9 below -52°C and morphology at 11, 13, 15 and 18 U.T.

Although the conditions proposed by Brunner et al. (2007a) were defined for GOES, they were considered applicable for images of the M-9, as the channels of both geostationary satellites are similar. The difference between the sensor of the GOES and that of the M-9 in the thermal infrared channel when estimating cloud-top brightness temperature is below one Kelvin (Gunshor et al., 2006; Schmit and Gunshor, 2007). The results obtained from the images of the section from 13 U.T. to 15 U.T. are presented in Table 2. We can observe that the 5 conditions are met in three of the nine analyzed time intervals (13:15 U.T., 13:45 U.T. and 14 U.T.), highlighting the image at 14 U.T., which has minimum temperature at the cloud-top registered and maximum temperature difference of the pair of cold-warm pixels. Although it would be necessary to have specific thresholds for the M-9, the obtained results were sufficiently distant from the GOES thresholds to consider that the small differences in values that might occur when using images of the M-9 instead of the GOES do not affect the detection of the V-shaped feature.

It must be said that compliance with these conditions is not synonymous with severe weather, but according to the results obtained by Brunner et al. (2007a), 91% of the 216 cases that met the determining factors were associated with severe weather (tornadoes, hail or strong winds not tornadoes). In our region, V-shaped feature associated with tornadoes in the Balearic Islands (Homar et al., 2001) and tornadoes (Aran et al., 2008) and floods (López and Aran, 2004) in Catalonia have been observed.

5 Internal structure of storms

5.1 Radar

The analysis of sequences of various radar products is presented as follows. The sequence of the product CAPPI (radar reflectivity at 1 km height) shows how one hour prior to the hailstorm in the Pla d'Urgell, convective cells lined up oriented from N to S in the west of the area. Their displacement was eastward and spreading southward, that is to say, new nuclei growing in that sector. Its maximum length (163 km at 14:54 U.T.) and the intensification of the precipitation occurred in the 14:45 U.T. and 15:12 U.T. periods (Figure 15).

The vertical development over the Pla d'Urgell area was more significant in the central-northern area than in the southern third (Figure 16). An outstanding feature of the storm was that the whole time there was little inclination towards vertical structure. That means that, apparently, there was little vertical decoupling of updrafts and downdrafts that favored an intensification of the rises. However, the TOP product (the height where 12 dBZ reflectivity is detected) had values between 14 and 15 km, quite a significant development to favor the formation of graupel and hail.

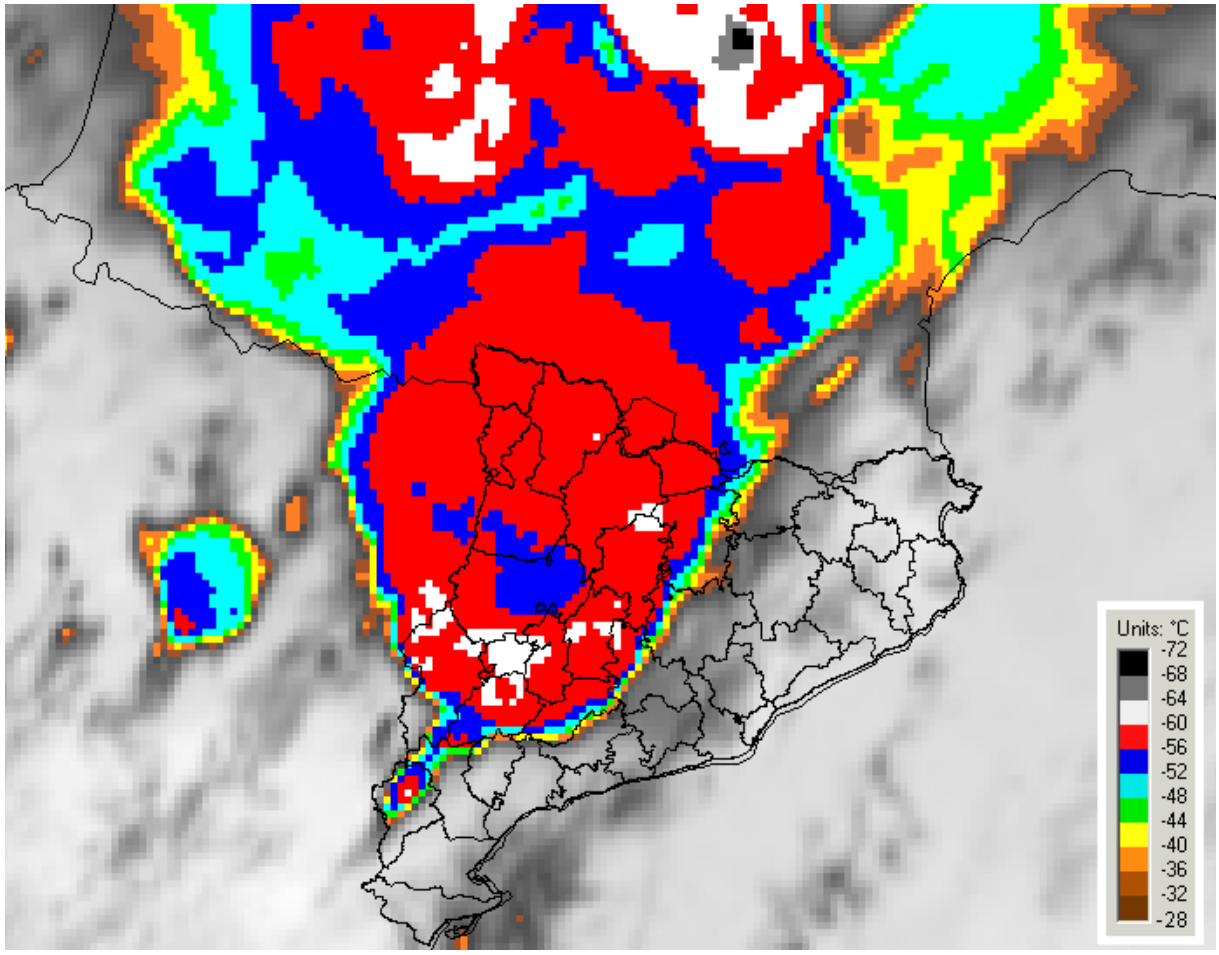

Figure 12. Color image from the IT channel of the M-9 at 14 U.T. The palette shows cloud-top brightness temperature with temperatures below -28°C, changing color every 4°C.

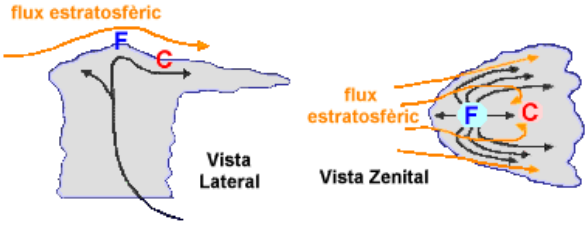

Figure 13. Schematic representation of overshooting and the coldest pixel (F), associated with overshooting, and the relatively warm pixel (C), associated with the small depression induced by the overshooting that is formed at leeward. Adapted from Heymsfield and Blackmer Jr. (1988).

Figure 17 shows how at 14:48 U.T. the more intense core was in the southwest of the Pla d'Urgell and that six minutes later the storm set off with intensity placing the maximum reflectivity near the ground (see the North - South and East - West projections of the reflectivity peaks in Figure 17).

A detailed study of the core that affected the Pla d'Urgell district (Figure 18) shows a very well formed V-notch structure in the south of Lleida at 14:36 U.T. Vertical developments were intensified (Figure 18c) in the southern sector while acquiring a more marked hook-shape at 14:48 U.T. (Figure 18a). At 14:54 U.T. this branch was broken in its northern sector. These shapes (structures) are characteristic features of cells associated with severe weather, specifically the supercells (Weisman and Klemp, 1986; Broyles et al., 2002). In order to find a mesocyclone in the hook area, Doppler radar images were analyzed, i.e., the radial velocity field of the precipitation in relation to the radar location. In Figure 19, the vertical cut made in the area where the largest hailstones fell (center of the Pla d'Urgell) contains a maximum of wind at low levels moving away from the radar and a line of change in wind direction. We can say that there was a cyclonic rotation, but it is difficult to say that there was a mesocyclone, as behind this maximum the signal is weak and not clear enough. Although there is no maximum detected in the north that is so localized, there is a transition zone in the direction of the wind.

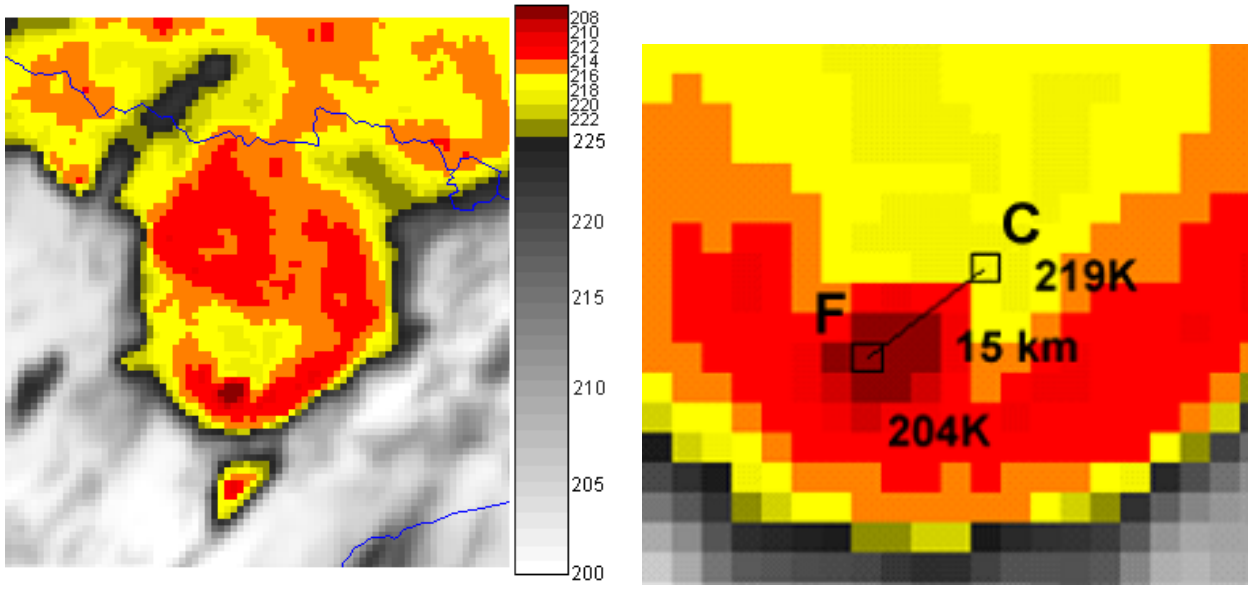

Figure 14. (a) (left) Detection of the signal in "V" in the IT channel of the M-9 at 14 U.T. (colored image) and (b) (right) extension of the overshooting zone of the image, with the detection of the pair of pixels cold (F) - warm (C). Temperatures in Kelvin.

Table 2. Results for the determining factors proposed by Brunner et al. (2007a) for the detection of the V-shaped feature for M-9 images from 13 to 15 U.T. At 13:25 U.T., 13:45 U.T. and 14 U.T. all conditions are right. The maximum values recorded in the images, which satisfy all the constraints are shown in bold.

	13	13:15	13:30	13:45	14	14:15	14:30	14:45	15
Overshooting	YES	YES	YES	YES	YES	YES	YES	YES	YES
Temp. colder pixel (K)	211	210	210	209	**204**	211	206	215	211
Temp. warmer pixel (K)	218	218	219	218	219	218	220	216	220
Temp. difference pair C-W	7	8	9	9	**15**	9	14	1	9
Distance couple C-W	19	11	10	15	15	37	11	43	21
Warm pixel within the V-shaped feature	NO	YES	NO	YES	YES	YES	NO	YES	YES

The VIL product (Vertical Integrated Liquid) (Greene and Clark, 1972) represents the amount of liquid water that the radar is able to detect in a column of the atmosphere. Thus, the larger liquid water content at the more elevated height, the higher VIL levels we will have and, therefore, the stronger updrafts to keep reflectivity values at upper levels (Martín et al., 2002). These conditions favor the formation and growth of meteors, and hence, the association VIL-hailstone. But it is necessary to keep in mind that this is not a one-to-one correspondence and that high values of VIL do not presuppose precipitation of graupel or hail (Martín et al., 2002). In the storm of the Pla d'Urgell, the area affected by a greater intensity of graupel and hail (number of impacts m^{-2}) corresponds to the areas where high values of VIL were observed (Figure 18b). In contrast, the correlation between the maximum VIL and the diameter of the hailstone is not so clear, because there is no spatial correspondence between the maximum, although the area affected by the hailstorm coincides with the areas in which the maximum of VIL were registered.

On 17/09/07 sustained values over 14 mm of VIL were reached for more than 30 minutes; values that are similar to other episodes of hailstorms with hailstones of considerable diameter (e. g. Martín et al., 2002). But to make a direct comparison of VIL values observed with other episodes is not always possible, as these can vary greatly depending on the season. According to Martín et al. (2002), autumn convective systems in the Mediterranean area present more significant precipitation echoes at lower levels than those attained in summer, resulting in very low VIL. Therefore, it is not possible to set a VIL threshold beyond which a convective cloud is a potential generator of hail. Despite these limitations, the radar is the parameter that in the present study case best corresponds spatially and temporally with the hailstone.

5.2 Lightning

Observation of severe weather on surface is usually preceded by an increase in the frequency of cloud-to-ground

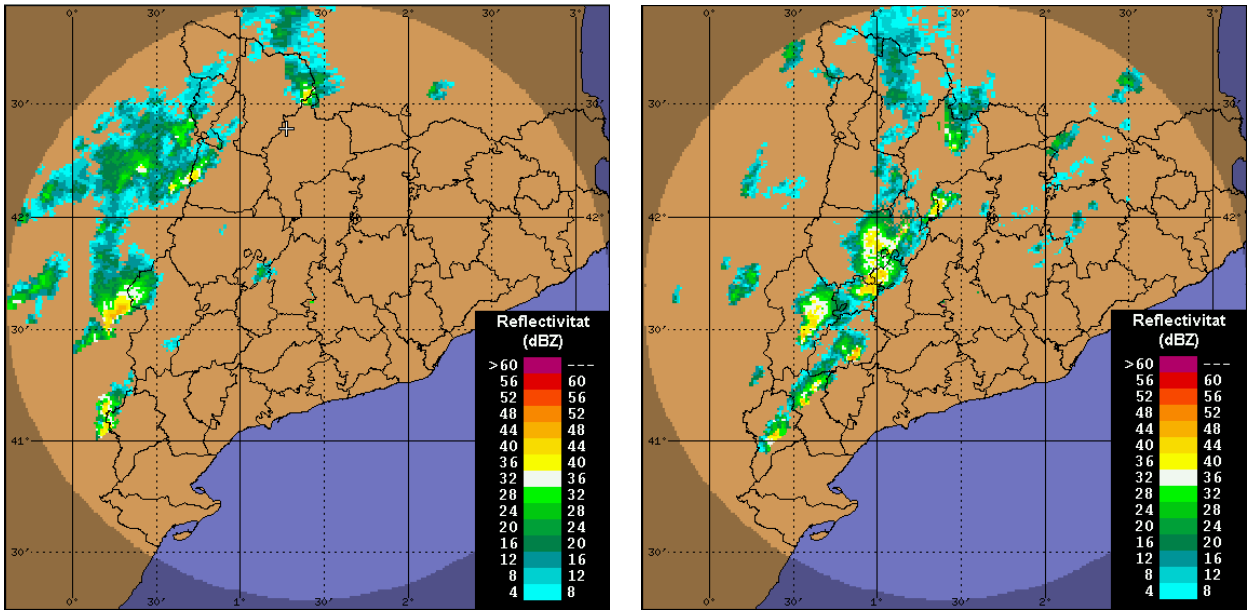

Figure 15. CAPPI product (radar reflectivity at 1 km height in dBZ) at (a) (left) 14:06 and (b) (right) 15:12 U.T. radar of La Creu del Vent.

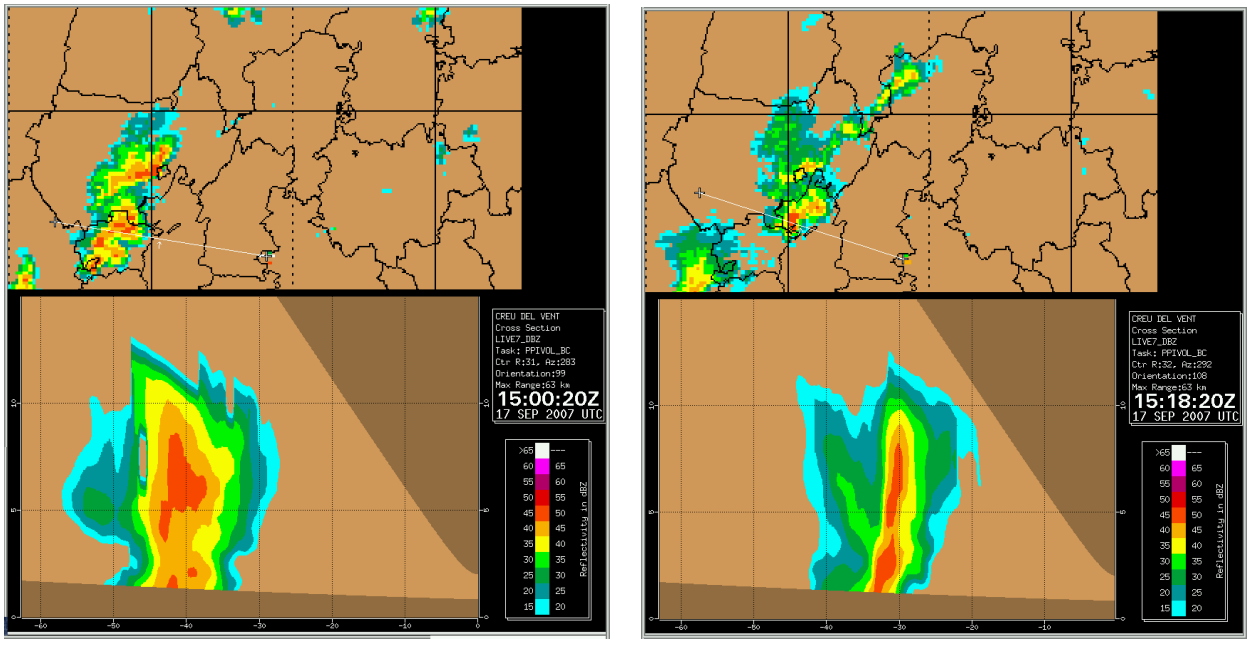

Figure 16. Vertical section of the radar reflectivity field (dBZ) (a) (left) in the area of the Pla d'Urgell to 15 U.T. and (b) (right) to the north of this region at 15:18 U.T. The transect (white line) of these cuts, which originated in the radar, are shown in the images above (CAPPI 1 km in dBZ).

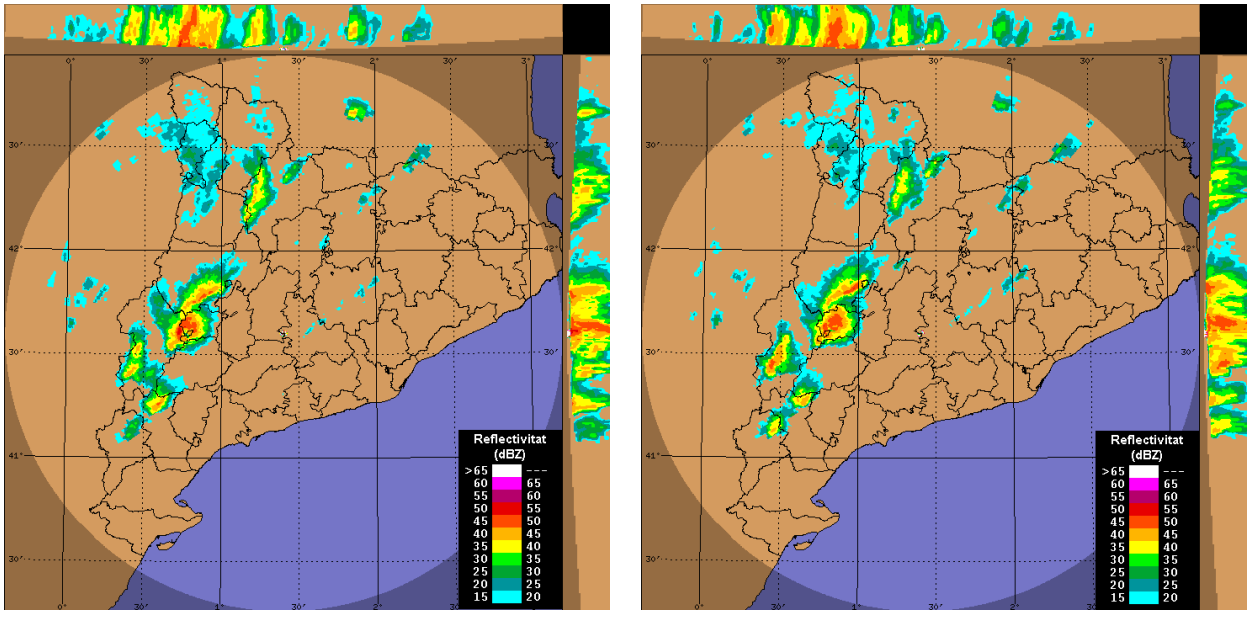

Figure 17. Reflectivity maximums and North-South and East-West projections at (a) (left) 14:48 U.T. and (b) (right) 14:56 U.T.

lightning (CG) (e. g. Changnon, 1992), although a high minute frequency is no guarantee of severe weather (Williams, 2001). Moreover, storms associated with severe weather may have anomalous electrical atmospheric behavior, either due to unusual values in the frequency of lightning or due to changes in the polarity of CG lightning. While the frequency of lightning is usually higher than in other storms (Williams, 2001), in some cases these severe storms have periods of their life cycle when the frequency of CG is considerably decreased. Regarding the polarity of lightning, there are severe storms that show a domain of positive polarity discharges (Carey and Rutledge, 1998; Soula et al., 2004; Wiens et al., 2005). This variety of behaviors in significant storms has to do with the complexity and degree of organization that they can achieve (Stolzenburg et al., 1998; Dotzek and Price, 2009).

As for hailstorms, Changnon (1992) studied the temporal and spatial relationship between lightning and hail. Regarding the temporal relationship, a temporal pattern between lightning and hail was observed, in which CG-lightning reached the maximum minute frequency about ten minutes before the observation of hail on surface. Furthermore, Changnon (1992) found that the intensity of the hailstorm could be related to the frequency of CG-lightning min-1 observed at the time of the hailstorm.

In the present case study, the time section between 14 at 16:30 U.T. was analyzed, selecting the lightning corresponding to the storm core that led to the hailstorm. This period of time covers most of the life cycle of the storm since its detection entering the Segrià until it dissipated in Berguedà.

During this period of two hours and a half, the XDDE recorded 9557 cloud-to-cloud lightning (CC) and 2096 CG lightning throughout the storm. The average frequency of total lightning (LT) (sum of CC and CG lightning) was 75 LT min^{-1}, with a maximum of 150 LT min^{-1} between 15:48 and 15:54 U.T. The average frequency of CG lightning was 13.4 CG min^{-1}, with a maximum of 19 CG min^{-1} between 14:54 and 15 U.T. These values are high and are comparable to the records of other storms associated with severe weather (Williams, 2001), exceeding 10 CG min^{-1}, a threshold that ordinary storms do not usually surpass (Lang et al., 2000).

To facilitate interpretation of the evolution of the frequency of lightning along the life cycle of the storm, it was analyzed together with the evolution of certain radar products Figure 20 shows the evolution of the LT, CC and CG lightning frequency, with the evolution of the Z_{max} (maximum reflectivity), the VIL and the TOP (height reached by radar reflectivity higher than 12 dBZ).

Initially, following the evolution of the total lightning, there are two peaks, a relative one at 14:54 U.T. (95 LT min^{-1}), and an absolute one at 15:48 U.T. (150 LT min^{-1}). The first LT peak corresponds approximately to the maximum of Z_{max} and VIL, while the absolute maximum LT does not coincide with any maximums of the mentioned products; the reflectivity and VIL have quite low values between 15:42 and the 15:54 U.T., during which the LT show values above 130 RT min^{-1}. This differential behavior around the two maximums of LT denotes two different phases of the storm. From 14:24 U.T., the LT as well as the VIL and the Z_{max} have some dramatic increases, peaking at 14:54 U.T., preceding the observations of surface hail. Then a progressive decline begins, which in the case of LT ends at 15:30 U.T., when its frequency is again sharply increased and reaches an absolute maximum at 15:48 U.T. when the storm was already over the Solsonès. In this second phase,

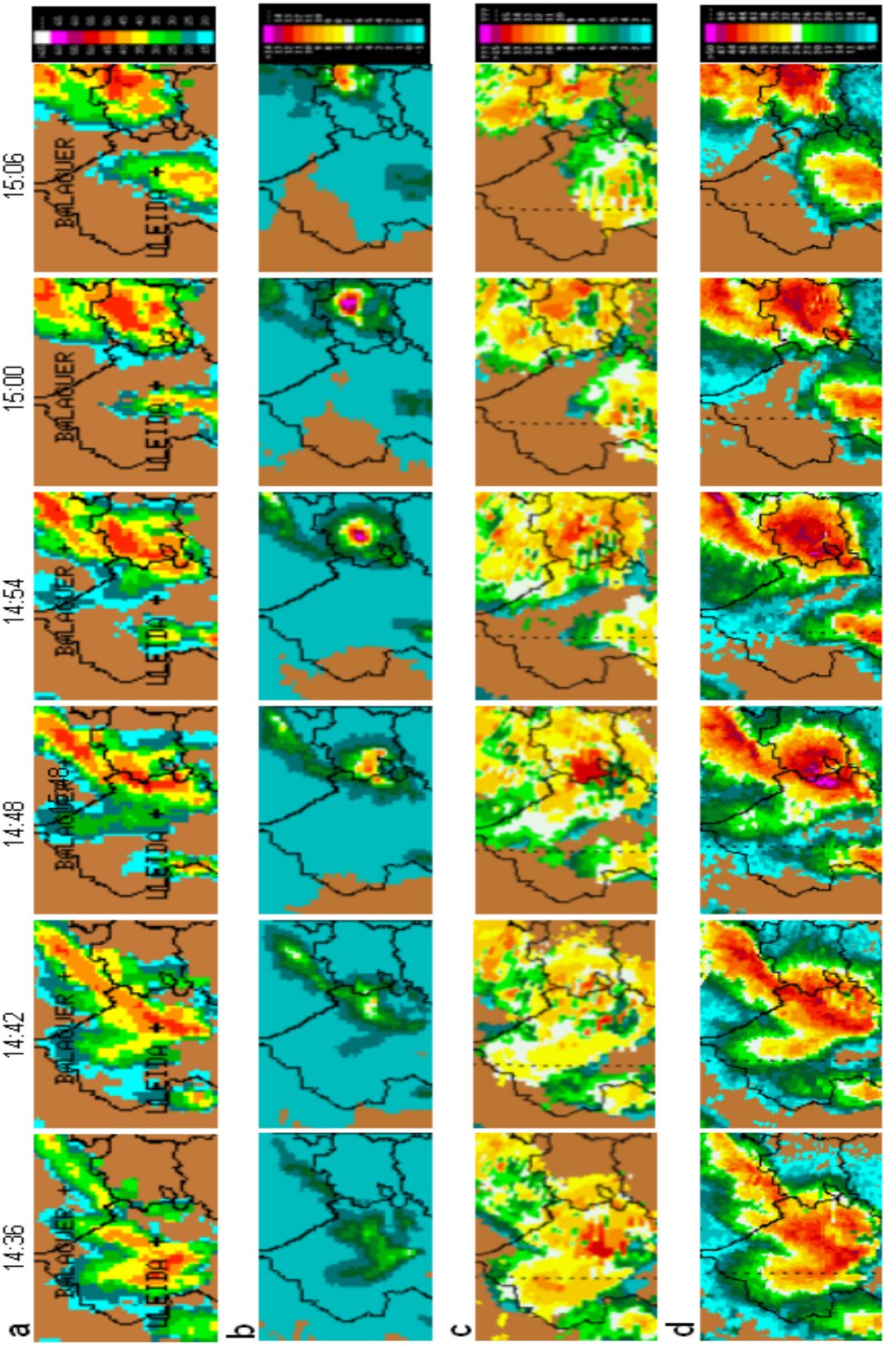

Figure 18. Radar image sequences in the study area from 14:36 until 15:06 U.T., according to the 6 minutes radar cycle. (a) CAPPI (radar reflectivity at 1 km altitude), (b) VIL (column of liquid water, in mm), (c) TOP (altitude reached by reflectivities above 12 dBZ) and (d) Z_{max} (maximum reflectivity in dBZ).

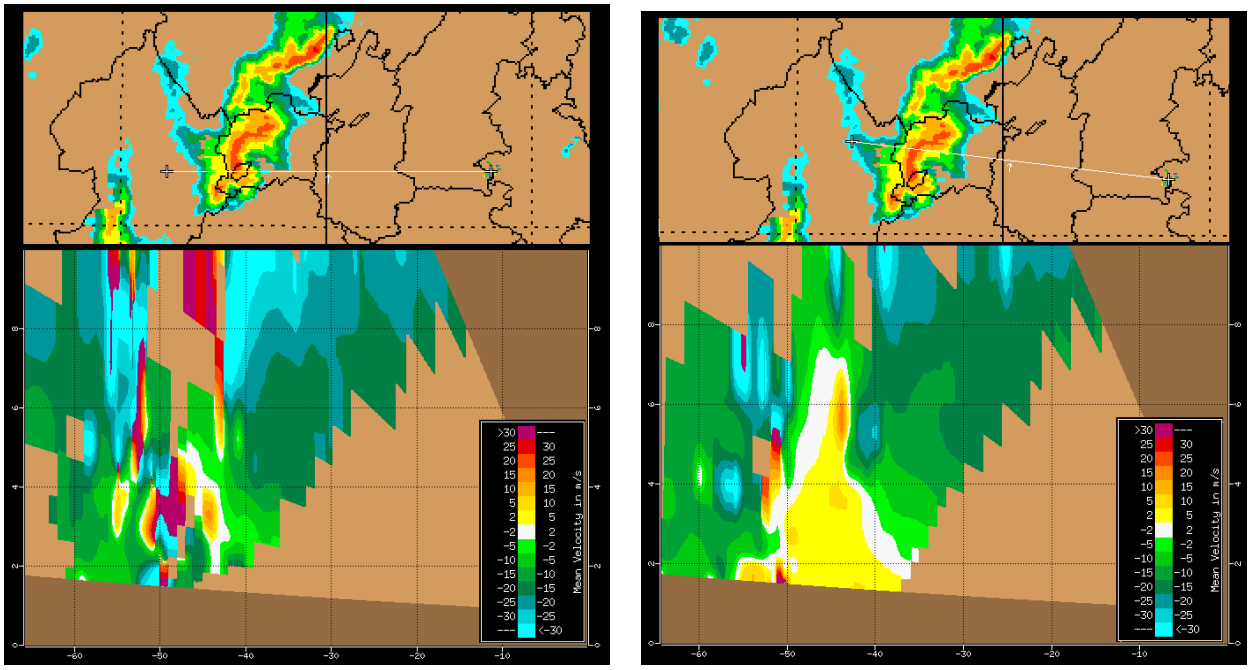

Figure 19. Vertical section of the radial velocity field of the radar in mode Doppler at 14:54 U.T. Transects (white line) of these cuts are shown in the images above (CAPPI 1 km).

unlike the first, neither the VIL nor the Z_{max} increase their values.

Continuing with the analysis of Figure 20, we can observe how the period with a high VIL (more than 11 mm between 14:48 and 15:12 U.T.) is displaced in time with respect to the period with a peak in Z_{max} (14:42 to 14:54 U.T.) and maximum frequency of LT lightning (more than 80 RT min^{-1} between 14:36 and 15 U.T.). The maximum of VIL is related to the time of the hailstorm and the displacement between the lightning maximum and the hailstorm corresponds to those observed in other episodes analyzed by Changnon (1992). In the second stage, the VIL also presents a relative maximum that is shifted with respect to the relative maximum of lightning, but with values well below those of the first phase, values which suggest that there was no hail precipitation in the second phase.

Concerning the evolution of the TOP, it remains at high values in the analyzed period, with over 13 km in height and just descends at the end of the analyzed time section (16:24 U.T.) when the storm is already in the dissipating stage. Unlike what happened with the Z_{max} and the VIL, where the evolution in relation with lightning showed different behaviors in both phases of the storm, the strong increases and LT maximums of the two phases occur during the two periods when TOP is at maximum (values above 15 km). In fact, the radar product that best correlates with the LT frequency is the TOP (Williams, 2001). This relationship has been studied for a long time (e. g. Byers and Braham, 1949), and has been shown to be exponential (Williams, 1985). Thus, small increments of TOP, when it already has high values, can have much more pronounced increases in the LT frequency, as seen in this study case, firstly from 14:24 U.T. and after, starting at 15:42 U.T., the moments when TOP is at maximum (15.2 km).

Rigo et al. (2008) analyzed the life cycle of the storms of 2006 in Catalonia from radar and lightning data. In the pattern of behavior that they present, the maximum frequency of LT-lightning occurs in the first half of the maturity stage of the storm, once it has reached a maximum vertical development and when reflectivity peaks are registered. In the hailstorm of 17/09/2007, the behavior differs from this pattern, since the highest lightning frequencies occur at the end of the maturity stage of the storm, just before the beginning of its dissipation. Comparing this case with the pattern of an ordinary storm seems as if the hail (the period of maximum VIL) adversely affects the CC-lightning generation, and the CC-ray frequency is recovered only when the solid precipitation ends.

We must say that the anomalous behavior of this storm is not the only one observed in storms with graupel or hail. Montanyà et al. (2007) analyzed two storms on 17 August 2004, one of which occurred near the present area of study, observing periods without CG lightning, while at the same time the radar reflectivities were high. In the second study, Montanyà et al. (2008) analyzed a hailstorm that left hailstones up to 40 mm in diameter at the Pla d'Urgell, on 16 June 2006, noting a large number of CG-lightning and a substantial reduction of discharges in the moments when the radar detected maximum reflectivity. These anomalous behaviors are linked

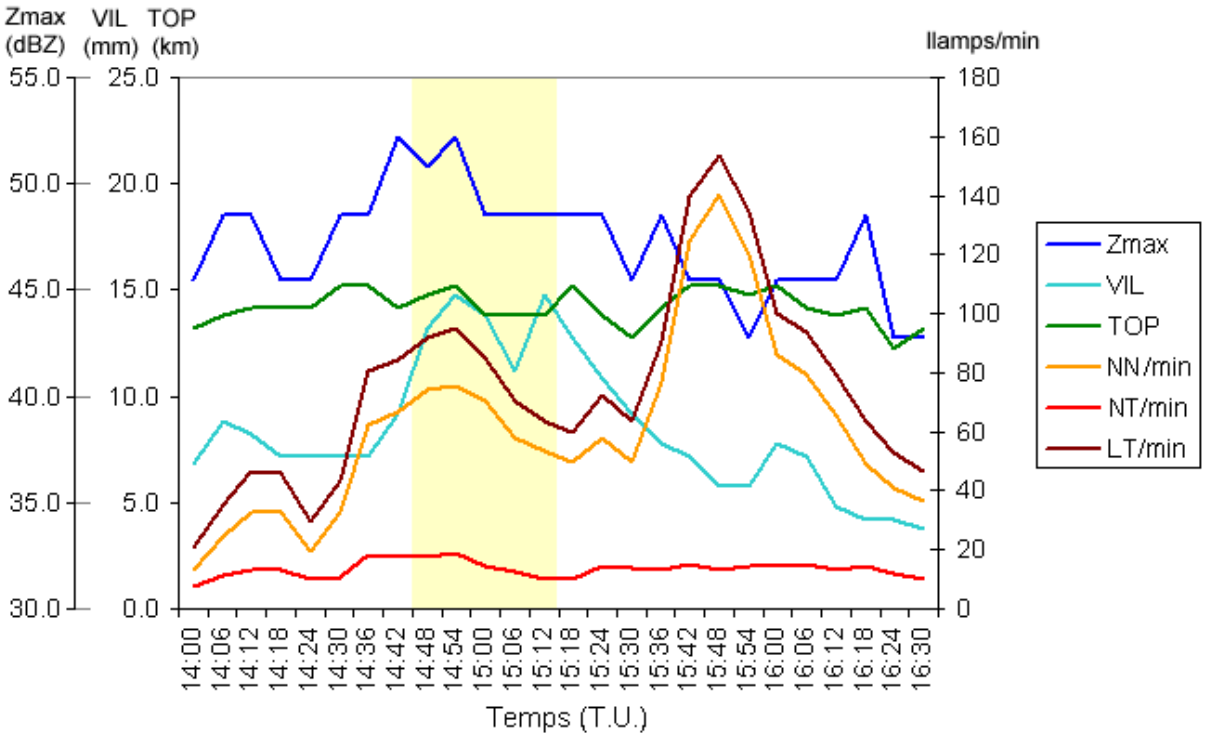

Figure 20. Evolution of the storm on 17/09/2007 between 14 U.T. and 16:30 U.T. Maximum radar reflectivity (Z_{max}), liquid water column (VIL), height of the reflectivity exceeding 12 dBZ (TOP product). Frequency of cloud-to-cloud lightning (NN), cloud-to-ground (NT) and total lightning (LT) (all of them according to their initials in Catalan) calculated every 6 minutes, coinciding with the cycle of radar images. The yellow shading corresponds to the period of the hailstorm.

to charge distributions within the clouds that do not follow standard patterns, such as storms with high charge (MacGorman et al., 1989) or storms with reverse polarity (Rust et al., 2005).

However, this analysis does not suggest that we are facing a storm with reverse polarity, as there was a normal proportion between polarities of CG-lightning, and also does not correspond with the hypothesis of heavy charge, because during the hailstorm the frequency of CG-lightning remains similar to the average of the analyzed period. The decrease of the CC frequency during precipitation was also observed by Montanyà et al. (2007), but the reason for this decrease is still unknown; although it might be related to a change in the electrical structure of the storm due to precipitation of hail.

6 Conclusions

The characterization of episodes of graupel/hail is important to establishing patterns of behavior that must allow a better identification of these phenomena. At a synoptic level, it is noteworthy that the episode occurred in conditions prone to produce graupel/hail in the area, with the presence of a trough at high levels. Both the analysis of low levels and the radiosonde reveal the presence of a dry layer on the Mediterranean coast. In this case the LSI index appears to be a good indicator when detecting the focused convention.

The analysis of the M-9 images allows the hailstorm episode to be catalogued within a mesoscale convective system. Furthermore, a V-shaped feature and a thermal dipole were detected, which is associated with the presence of severe weather on surface. The detection of this type of feature in real-time on M-9 images can be interesting as a tool for short-term prognosis.

Regarding the radar, characteristic features of supercells were detected, but despite the cyclonic rotation we cannot say that it was associated with a mesocyclone. The VIL product showed values comparable to other episodes of graupel/hail. In addition, the VIL is the analyzed radar product that best permits definition of the area affected by the meteor, despite not having a sufficiently defined relation with the size of the stone.

Analysis of the atmospheric electrical activity of the storm shows a high average frequency of both cloud-to-cloud lightning and cloud-to-ground lightning, comparable to frequencies reported in other storms associated with severe weather.

The analysis of the life cycle combining radar products and lighting shows that this case study does not follow a regular storm pattern, as the storm can be divided into two phases with different behaviors. The first phase is the hailstorm on the Pla d'Urgell, a period during which the peaks of Z_{max}, VIL, TOP-ray and high lightning frequencies are recorded. The second phase is characterized by a higher lightning frequency, high TOP and Z_{max} and VIL

values significantly lower than those recorded in the first phase.

Acknowledgements. The authors of this paper want to thank the contribution of colleagues in the SMC, particularly Tomeu Rigo, Roger Bordoy, Joan Bech, Abdelmalik Sairouni and Manel Bravo. We also want to say thank you for the work done by the *ADV Terres de Ponent*. Finally we want to thank the reviewers for their comments, which have improved this study.

References

Adler, R. F. and Mack, R. A., 1986: *Thunderstorm cloud top dynamics as inferred from satellite observations and a cloud top parcel model*, J Atmos Sci, **43**, 1945–1960.

Aran, M., Sairouni, A., Bech, J., Toda, J., Rigo, T., Cunillera, J., and Moré, J., 2007: *Pilot project for intensive surveillance of hail events in Terres de Ponent (Lleida)*, Atmos Res, **83**, 315–335.

Aran, M., Amaro, J., Arús, J., Bech, J., Figuerola, F., Gayà, M., and Vilaclara, E., 2008: *Synoptic and mesoscale diagnosis of a tornado event in Castellcir, Catalonia, on 18th October 2006*, Atmos Res, p. DOI:10.1016/j.atmosres.2008.10.016.

Atkins, N. T., Weisman, M. L., and Wicker, L. J., 1999: *The Influence of Preexisting Boundaries on Supercell Evolution*, Mon Wea Rev, **127**, 2910–2927.

Augustine, J. and Howard, K. W., 1988: *Mesoscale convective complexes over the United States during 1985*, Mon Weather Rev, **116**, 685–701.

Augustine, J. and Howard, K. W., 1991: *Mesoscale convective complexes over the United States during 1986 and 1987*, Mon Weather Rev, **119**, 1575–1589.

Bech, J., Vilaclara, E., Pineda, N., Rigo, T., López, J., O'Hora, F., Lorente, J., Sempere, D., and Fàbregas, F. X., 2004: The weather radar network of the Catalan Meteorological Service: description and applications, Proceedings of ERAD (2004): 416-420, Copernicus GmbH.

Bluestein, H. B., 1986: Fronts and jet streaks. A Mesoscale Meteorology and Forecasting, P.S (Ed.), Amer Meteor Soc, Boston, MA, 173-215.

Broyles, C., Wynne, R., Dipasquale, N., Guerrero, H., and Hendricks, T., 2002: Radar characteristics of violent tornadic storms using the NSSL algorithms across separate geographic regions of the United States, Proceedings of the 21st Conf. on Severe Local Storms, AMS, San Antonio, Texas, august 12-16.

Brunner, J. C., Ackerman, S. A., Bachmeier, A. S., and Rabin, R. M., 2007a: *A Quantitative Analysis of the Enhanced-V Feature in Relation to Severe Weather*, Wea Forecasting, **22**, 853–872.

Brunner, J. C., Feltz, W., Ackerman, S., Moses, J., and Rabin, R. M., 2007b: Toward An Objective Enhanced-V Detection Algorithm, Proceedings of the Joint 2007 EUMETSAT Meteorological Satellite Conference and the 15th Satellite Meteorology & Oceanography Conference of the American Meteorological Society, Amsterdam, The Netherlands, september 24-28.

Byers, H. R. and Braham, R. R., 1949: The thunderstorms, U.S. Government Printing Office, 282 pp.

Carey, L. D. and Rutledge, S. A., 1998: *Electrical and multiparameter radar observations of a severe hailstorm*, J Geophys Res, **103**, 13 979–14 000.

Ceperuelo, M., Rigo, T., San Ambrosio, I., and Llasat, M. C., 2006: Estudio de dos granizadas severas registradas en 2004 en el Llano de Lleida, XXIX Jornadas Científicas de la Asociación Meteorológica Española, Pamplona.

Changnon, S. A., 1992: *Temporal and spatial relations between hail and lightning*, J Appl Meteor, **31**, 587–604.

Corfidi, S. F., 2003: *Cold pools and MCS propagation: forecasting the motion of downwind-developing MCSs*, Wea Forecasting, **18**, 997–1017.

Correoso, J. F., Hernández, E., García-Herrera, R., Barriopedro, D., and Paredes, D., 2006: *A 3-year study of cloud-to-ground lightning flash characteristics of Mesoscale convective systems over the Western Mediterranean Sea*, Atmos Res, **79**, 89–107.

Davies, J. M., 2004: *Estimations of CIN and LFC associated with tornadic and nontornadic supercells*, Wea Forecasting, **19**, 714–726.

Dotzek, N. and Price, C., 2009: Lightning Characteristics of Extreme Events. A Lightning: Principles, Instruments and Applications, Betz, H.-D., Schumann, U., Laroche, P. (eds.), Springer, pp. 487-508.

Farnell, C., Aran, M., Andrés, A., Busto, M., Pineda, N., and Torà, M., 2009: *Estudi de la pedregada del 17 de setembre de 2007 al Pla d'Urgell. Primera part: Treball de camp i anàlisi dels granímetres*, Tethys, **6**.

Font, I., 1983: Climatología de España y Portugal, Instituto Nacional de Meteorología, Madrid, 269 pp.

Fujita, T. T., 1978: Manual of downburst identification for project NIM-ROD, SMPR 156, University of Chicago, 104 pp.

García-Ortega, E., Fita, L., Romero, R., López, L., Ramis, C., and Sánchez, J. L., 2007: *Numerical simulation and sensitivity study of a severe hailstorm in northeast Spain*, Atmos Res, **83**, 225–241.

Graziano, T. M. and Carlson, T. N., 1987: *A Statistical Evaluation of Lid Strength on Deep Convection*, Wea Forecasting, **2**, 127–139.

Greene, D. R. and Clark, R. A., 1972: *Vertically integrated liquid water - A new analysis tool*, Mon Wea Rev, **100**, 548–552.

Gunshor, M. M., Schmit, T. J., Menzel, W. P., and Tobin, D. C., 2006: Intercalibration of the newest geostationary imagers via high spectral resolution AIRS data, 14th Conference on Satellite Meteorology and Oceanography, Atlanta, GA, American Meteorological Society.

Heymsfield, G. M. and Blackmer Jr., R. H., 1988: *Satelliteobserved characteristics of Midwest severe thunderstorm anvils*, Mon Wea Rev, **116**, 2200–2224.

Holleman, I., 2001: Hail detection using single-polarization radar, Scientific report WR-2001-01, Royal Netherlands Meteorological Institute (KNMI).

Homar, V., Gayà, M., and Ramis, C., 2001: *A synoptic and mesoescale diagnosis of a tornado outbreak in the Balearic Islands: phenomena and environment characterization*, Atmos Res, **56**, 253–267.

Jirak, I. L., Cotton, W. R., and McAnelly, R. L., 2003: *Satellite and Radar Survey of Mesoscale Convective System Development*, Mon Wea Rev, **131**, 2428–2449.

Kurino, T., 1996: A Rainfall Estimation with the GMS-5 Infrared Split-Window and Water Vapour Measurements, Tech. Rep., Meteorological Satellite Centre, Japan Meteorological Agency.

Lang, T. J., Rutledge, S. A., Dye, J. E., Venticinque, M., Laroche, P., and Defer, E., 2000: *Anomalously low negative cloud-to-ground lightning flash rates in intense convective storms observed during*

STERAO-A, Mon Wea Rev, **128**, 160–173.

López, J. M. and Aran, M., 2004: Estudio de una ciclogénesis rápida mediterránea: Cataluña, 9-10 de junio de 2000, Nota Técnica del CMT de Cataluña, Instituto Nacional de Meteorología, 108 pp.

MacGorman, D. R., Burgess, D. W., Mazur, V., Rust, W. D., Taylor, W. L., and Johnson, B. C., 1989: *Lightning rates relative to tornadic storm evolution on 22 May 1981*, J Atmos Sci, **46**, 221–250.

Maddox, R. A., 1980: *Mesoscale convective complexes*, Bull Amer Meteor Soc, **61**, 1374–1387.

Maddox, R. A., Howard, K. W., Bartels, D. L., and Rodgers, D. M., 1986: Mesoscale convective complexes in the middle latitudes. A Mesoscale Meteorology and Forecasting, American Meteorological Society, Boston, pp. 390-413.

Martín, F., San Ambrosio, I., and Carretero, O., 2002: Supercélula severa en el área mediterránea, Nota técnica del STAP núm. 37, Instituto Nacional de Meteorología, 174 pp.

McCann, D. W., 1983: *The Enhanced-V: A satellite observable severe storm signature*, Mon Wea Rev, **111**, 887–894.

Montanyà, J., Soula, S., and Pineda, N., 2007: *A study of the total lightning activity in two hailstorms*, J Geophys Res, **112**, DOI: 10.1029/2006JD007 203.

Montanyà, J., Soula, S., Pineda, N., van der Velde, O., Clapers, P., Solà, G., Bech, J., and Romero, D., 2008: *Study of the total lightning activity in a hailstorm*, Atmos Res, **91**, DOI: 10.1016/j.atmosres.2008.06.008.

Pascual, R., 2002: Estudio de las granizadas en el llano de Lleida, Nota técnica núm. 3, Centro Meteorológico Territorial de Catalunya, Instituto Nacional de Meteorología, http://www.aemet.es/es/divulgacion/varios/detalles/biblioteca_tempoweb.

Pineda, N. and Montanyà, J., 2009: Lightning Detection in Spain: The Particular Case of Catalonia. A Lightning: Principles, Instruments and Applications, Betz, H.-D., Schumann, U., Laroche, P. (eds.), Springer, pp. 161-185.

Ramis, C., López, J. M., and Arús, J., 1999: *Two cases of severe weather in Catalonia (Spain): A diagnostic study*, Meteor Appl, **6**, 11–27.

Richard, P. and Lojou, J. Y., 1996: Assessment of application of storm cell electrical activity monitoring to intense precipitation forecast, Proceedings of the 10th International Conference on Atmospheric Electricity, Osaka, Japan, june, 284-287.

Rigo, T., Pineda, N., and Bech, J., 2008: Estudi i modelització del cicle de vida de les tempestes amb tècniques de teledetecció, Nota d'Estudi, Servei Meteorològic de Catalunya, 72, 56 pp.

Rust, W. D., MacGorman, D. R., Bruning, E. C., Weiss, S. A., Krehbiel, P. R., Thomas, R. J., Rison, W., Hamlin, T., and Harlin, J., 2005: *Inverted-polarity electrical structures in thunderstorms in the Severe Thunderstorm Electrification and Precipitation Study (STEPS)*, Atmos Res, **76**, 247–271.

Sánchez, J. L., Fernández, M., Pastor, F., and Estrela, M. J., 2001: Analysis of heavy precipitation in the region of Valencia (Spain) by means of IR images from the Meteosat, Proceedings of "Symposium on Precipitation Extremes: Prediction, Impacts and Responses", American Meteorological Society, Albuquerque, New Mexico, pp. 166- 169.

Sánchez, J. L., Fernández, M. V., Fernández, J. T., Tudurí, E., and Ramis, C., 2003: *Analysis of mesoscale convective systems with hail precipitation*, Atmos Res, **67-68**, 573–588.

Schmit, T. J. and Gunshor, M. M., 2007: Intercalibrating the world's geostationary imagers via polar orbiting high spectral resolution data, Joint 2007 EUMETSAT Meteorological Satellite Conference and the 15th Satellite Meteorology & Oceanography Conference of the American Meteorological Society, Amsterdam, the Netherlands, september.

Soula, S., Seity, Y., Feral, L., and Sauvageot, H., 2004: *Cloud-to-ground lightning activity in hail-bearing storms*, J Geophys Res, **109**, DOI: 10.1029/ 2003JD003 669.

Stolzenburg, M., Rust, W. D., and Marshall, T. C., 1998: *Electrical structure in thunderstorm convective regions. 3. Synthesis*, J Geophys Res, **103**, 14 097–14 108.

Tudurí, E., Romero, R., López, L., García, E., Sánchez, J. L., and Ramis, C., 2003: *The 14 July 2001 hailstorm in northeastern Spain: diagnosis of the meteorological situation*, Atmos Res, **67-68**, 541–558.

Veciana, R., Pineda, N., Bech, J., and Miró, A., 2003: Monitoring deep convection with a satellite overshooting analysis technique, 5th Plinius Conference on Mediterranean Storms, Ajaccio, Corsica, France, october.

Wang, P. K., 1997: *The thermodynamic structure atop a penetrating convective thunderstorm*, Atmos Res, **83**, 254–262.

Weisman, M. L. and Klemp, J. B., 1986: Characteristics of isolated convective storms, A Mesoscale Meteorology and Forecasting, Ray, P. S. (Ed), American Meteorological Society, 331-358.

Wiens, K. C., Rutledge, S. A., and Tessendorf, S. A., 2005: *The 29 June 2000 supercell observed during STEPS. Part II: lightning and charge structure*, J Atmos Sci, **62**, 4151–4177.

Williams, E. R., 1985: *Large scale charge separation in thunderclouds*, J Geophys Res, **90**, 6013–6025.

Williams, E. R., 2001: *The electrification of severe storms*, Meteorological Monographs, **28**, 527–561.